Supporting Information for

Electrochemical Generation of an Open-Shell Gold(III)–Dithiolene Porous Coordination Polymer

Yohan Cheret,[1] Ghenadie Novitchi,[2] Kaoutar Benjelloun,[1] Pascale Auban-Senzier,[3] Pere Alemany,[4] Enric Canadell,*[,5] Narcis Avarvari,*[,1] Nicolas Zigon*[,1]

[1] Univ Angers, CNRS, MOLTECH-ANJOU, SFR MATRIX, F-49000 Angers, France. E-mail: narcis.avarvari@univ-angers.fr ; nicolas.zigon@univ-angers.fr

[2] Laboratoire National des Champs Magnétiques Intenses, Université de Grenoble Alpes, INSA Toulouse, Université de Toulouse Paul Sabatier, EMFL, CNRS, 25 avenue des Martyrs, 38042 Grenoble, France

[3] Université Paris-Saclay, CNRS, UMR 8502, Laboratoire de Physique des Solides, 91405 Orsay, France

[4] Departament de Ciència de Materials i Química Física and Institut de Química Teòrica i Computacional (IQTCUB), Universitat de Barcelona, Martí i Franquès 1, 08028 Barcelona, Spain

[5] Institut de Ciència de Materials de Barcelona, ICMAB-CSIC, Campus de la UAB, 08193 Bellaterra, Spain, and Royal Academy of Sciences and Arts of Barcelona, Chemistry Section, La Rambla 115, 08002 Barcelona, Spain. E-mail: canadell@icmab.es

Summary

Experimental Part

All reagents and chemicals commercially available were used without further purification. Solvents were dried using standard techniques. NMR spectra were recorded on a Bruker III 300 (^{1}H, 300 MHz ; ^{13}C, 75 MHz). Chemical shifts are given in parts per million (ppm) relative to TMS and coupling J in Hertz (Hz). High resolution mass spectrometry (HRMS) was performed with Jeol JMS-S3000 SpiralTOF. Cyclic voltammetry was performed using a Biologic SP-150 potentiostat with positive feedback compensation. Tetrabutylammonium hexafluorophosphate (0.1 M as supporting electrolyte) was purchased from Sigma-Aldrich and recrystallized prior to use. Experiments were carried out in a one-compartment cell equipped with platinum working microelectrode (Ø = 2 mm) and a platinum wire counter electrode. A silver wire immersed in 0.01M $AgNO_3$ acetonitrile solution was used as pseudo-reference electrode and checked against ferrocene/ferrocenium couple (Fc/Fc^{+}) before and after each experiment. Single crystals of the compounds were mounted on glass fibre loops using a viscous hydrocarbon oil to coat the crystal and then transferred directly to cold nitrogen stream for data collection. Data collection were mostly performed on an Agilent Supernova with CuKα radiation (λ = 1.54184 Å). The structures were solved by intrinsic phasing and refined on F^2 by full matrix least-squares techniques with SHELX programs (SHELXT 2018/2 and SHELXL 2018/3)[1,2] using the ShelXle and the Olex2 graphical user interfaces.[3,4] These data can be obtained free of charge from CCDC, 12 Union road, Cambridge CB2 1EZ, UK with the deposition numbers **2532706-2532708** (e-mail: deposit@ccdc.cam.ac.uk or http://www.ccdc.cam.ac.uk/.

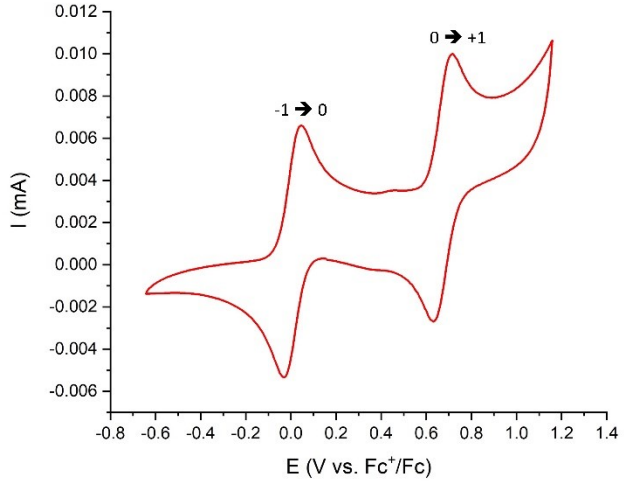

Figure S 1. Cyclic Voltammogram for **1-Bu$_4$$^-$;TBA$^+$** (DCM, C = 1·10^{-3} mol.L^{-1}, $TBAPF_6$ 0.1 M, Ar, WE and CE = Pt, RE = Ag^+/Ag).

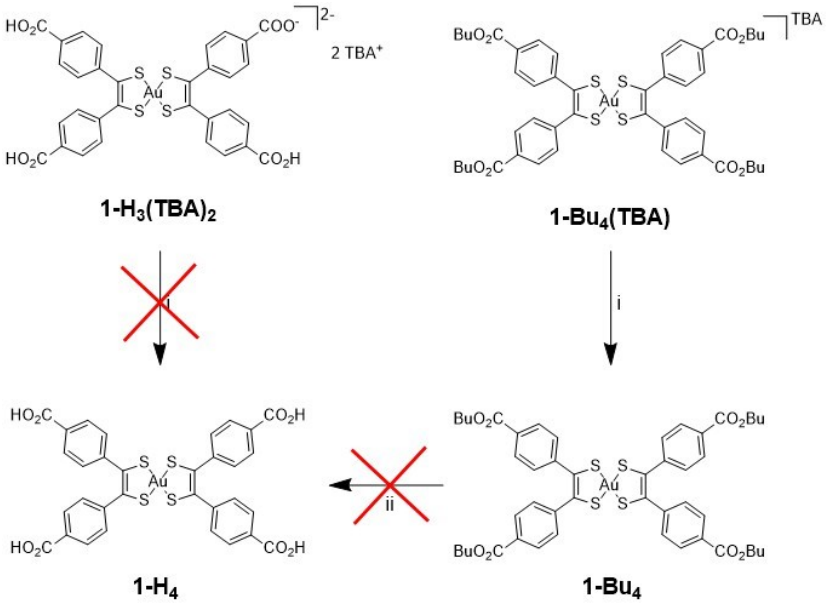

Scheme S 1. Synthetic trials to obtain the target neutral Au-dithiolene complexes **1-H$_4$**. i) I_2, CH_2Cl_2, ii) TBAOH, THF, H_2O.

$$\chi_c = \frac{N_A g^2 \mu_B^2}{kT} \frac{0.25 + 0.14995\,x + 0.30094\,x^2}{1.0 + 1.9862\,x + 0.68854\,x^2 + 6.0626\,x^3}$$

$$x = \frac{|J|}{kT}$$

Equation S 1. Analytical expression for the magnetic susceptibility of a regular 1D chain.

$$\chi = \chi_c(1-\rho) + \rho \frac{N_A g_i^2 \mu_B^2}{3kT} S(S+1)$$

Equation S 2. Expression of the total magnetic susceptibility accounting for the presence of Curie-type magnetic defects.

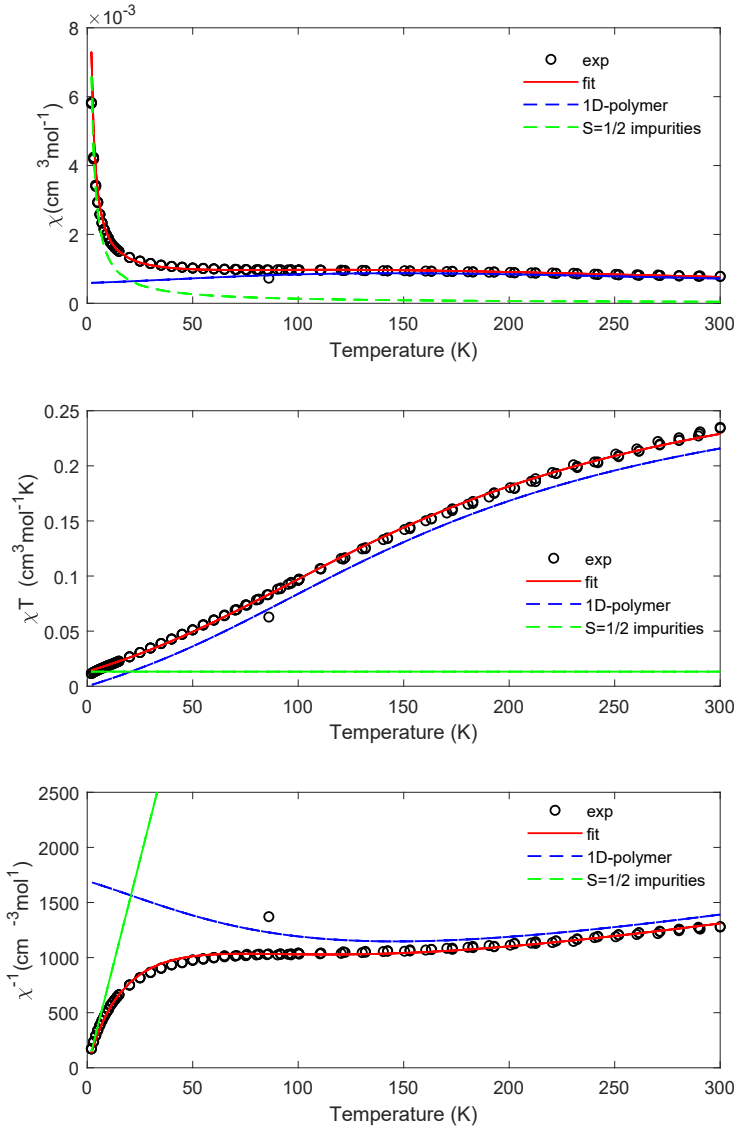

Figure S 2. Experimental magnetic data for **1-Cd$_2$** (black circles) together with the best-fit curves (red lines) for the temperature dependence of χ, χT, and 1/χ. The blue line represents the contribution of the polymeric 1D chain, while the green line corresponds to the Curie-type contribution from isolated S = 1/2 spins with g=2.0.

Table S 1. *Crystallographic data, details of data collection and structure refinement parameters.*

	1-Bu$_4$	**1-H$_3$(TBA)$_2$**	**1-Cd$_2$**
Formula sum	$C_{48.50}H_{52.50}AuN_{0.25}O_8S_4$	$C_{64}H_{91}AuN_2O_8S_4$	$C_{34.25}H_{23.25}AuCd_2N_{0.75}O_{10}S_4$
Formula weight	1092.11	1341.59	1155.29
Crystal system	Triclinic	Monoclinic	Hexagonal
Space group	*P*-1	$P2_1/c$	$P6_5$
a/Å	15.5973(3)	21.1317(3)	19.51040(10)
b/Å	25.2395(5)	9.43303(10)	19.51040(10)
c/Å	26.4393(5)	17.6654(2)	20.2619(2)
α/°	104.210(2)	90	90
β/°	94.801(2)	111.9150(14)	90
γ/°	101.498(2)	90	120
V/Å^3	9790.5(3)	3266.89(7)	6679.49(10)
Z / Z'	2 / 4	4 / 0.5	6 / 1
D_c/g cm^{-3}	1.482	1.364	1.723
T/K	200.00(10)	293.0(9)	295.4(3)
μ/mm^{-1}	7.652	5.839	15.814
Reflections (total)	37746	5844	9299
final $R_1{}^a$, $wR_2{}^b$ [$I > 2\sigma(I)$]	0.0955/0.2552	0.0659/0.1588	0.0298/0.0777
$R_1{}^a$,$wR_2{}^b$ (all data)	0.1139/0.2764	0.0686/0.1649	0.0319/0.0797
goodness-of-fit on F^2	1.042	1.066	1.049
$\Delta\rho_{min}/\Delta\rho_{max}$ (e Å^{-3})	-2.360/3.186	-2.130/3.243	-0.838/0.869
Completeness (%)	99.9	98.4	99.6
Flack (Parsons)	-	-	-0.023(5)
CCDC number	2532708	2532707	2532706

Atom 1	Atom 2	Length (Å)	Atom 1	Atom 2	Length (Å)
Au1A	S4A	2.295(3)	Au1B	S3B	2.305(3)
Au1A	S1A	2.283(3)	Au1B	S4B	2.285(2)
Au1A	S2A	2.296(3)	Au1B	S1B	2.295(3)
Au1A	S3A	2.291(3)	Au1B	S2B	2.289(2)
S1A	C13A	1.72(1)	S2B	C25B	1.74(1)
S2A	C14A	1.75(1)	S1B	C24B	1.73(1)
S4A	C37A	1.76(1)	S4B	C12B	1.71(1)
S3A	C38A	1.75(1)	S3B	C13B	1.72(1)
C13A	C14A	1.35(2)	C13B	C12B	1.39(2)
C37A	C38A	1.37(2)	C24B	C25B	1.36(2)
Atom 1	**Atom 2**	**Length (Å)**	**Atom 1**	**Atom 2**	**Length (Å)**
Au1C	S3C	2.283(2)	Au1D	S2D	2.301(3)
Au1C	S4C	2.303(3)	Au1D	S3D	2.284(3)
Au1C	S1C	2.285(2)	Au1D	S4D	2.299(3)
Au1C	S2C	2.297(3)	Au1D	S1D	2.295(3)
S2C	C26C	1.78(1)	S1D	C11D	1.73(1)
S1C	C25C	1.73(1)	S2D	C12D	1.74(1)
S4C	C12C	1.78(1)	S4D	C34D	1.74(1)
S3C	C13C	1.73(1)	S3D	C35D	1.71(1)
C12C	C13C	1.37(2)	C11D	C12D	1.35(2)
C25C	C26C	1.38(1)	C34D	C35D	1.40(2)

Table S 2. Selected bond lengths for **1-Bu$_4$**.

Atom 1	Atom 2	Length (Å)
Au1	S2	2.316
Au1	S1	2.303
S1	C13	1.769(4)
S2	C19	1.768(4)
C13	C19	1.347(6)

Table S 3. Selected bond lengths for **1-H$_3$(TBA)$_2$**.

Atom 1	Atom 2	Length (Å)
Au2	S1	2.277(2)
Au2	S2	2.279(2)
Au2	S3	2.282(2)
Au2	S4	2.281(2)
S4	C25	1.723(9)
S3	C26	1.738(9)
S1	C8	1.724(7)
S2	C9	1.740(9)
C8	C9	1.36(2)
C26	C25	1.36(2)

Table S 4. Selected bond lengths for **1-Cd$_2$**.

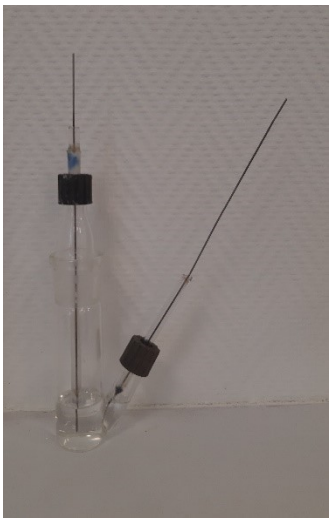

Figure S 3. Set-up used for the electrocrystallization of **1-Cd$_2$.**

Figure S 4. Microscope picture of the crystals obtained from the solvothermal electrocrystallization of **1-Cd$_2$** (red arrows : crystalline dark needles of **1-Cd$_2$** : red arrows ; yellow **1-Cd$_2$(TBA)** : green arrows).

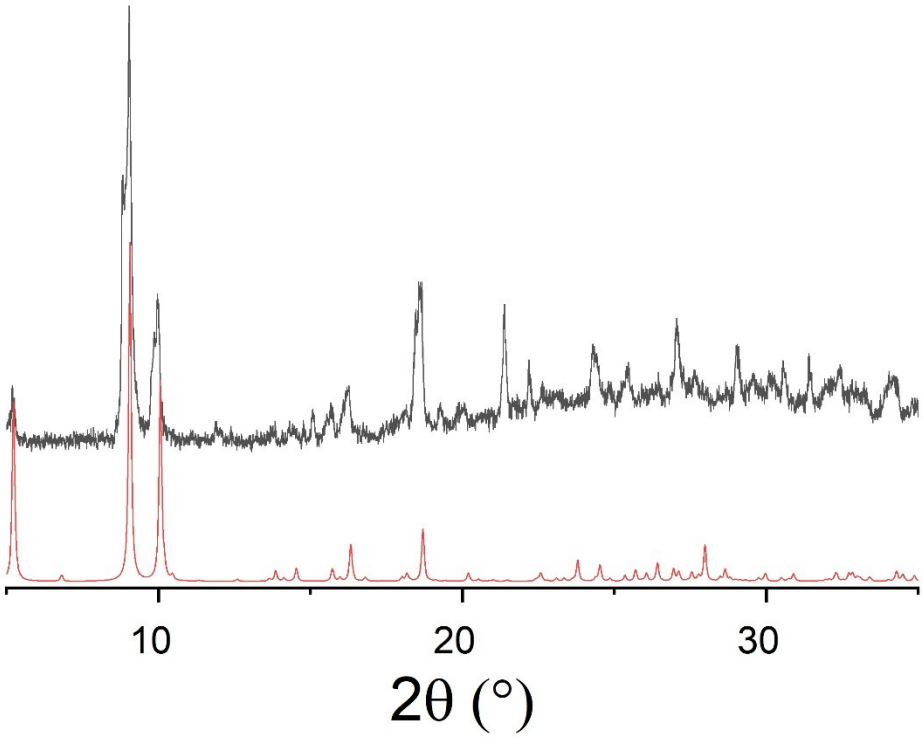

Figure S 5. Powder X-Ray Diffractogram of **1-Cd$_2$** (red : simulated ; black : experimental).

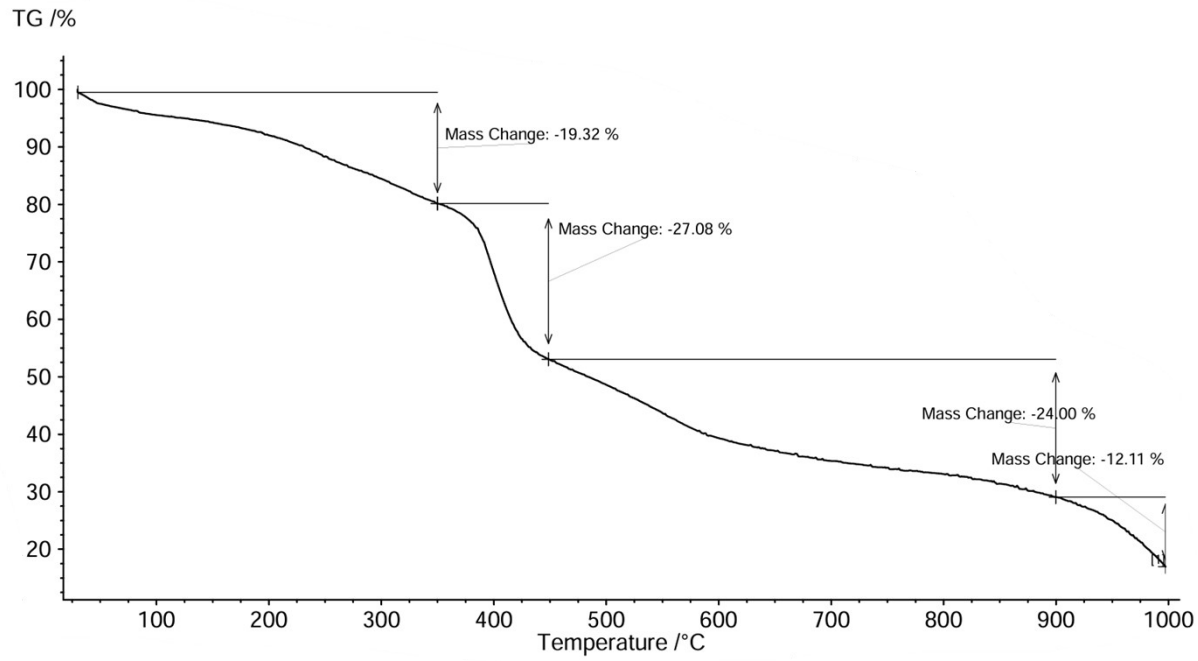

Figure S 6. TGA of **1-Cd$_2$** (Argon flow, 10 K/min scan-rate). The loss of the solvent (DMF, EtOH, acetone or water) is observed until 330°C. The material is degraded above 350°C. At 900°C, the remaining mass corresponds to the inorganic parts.

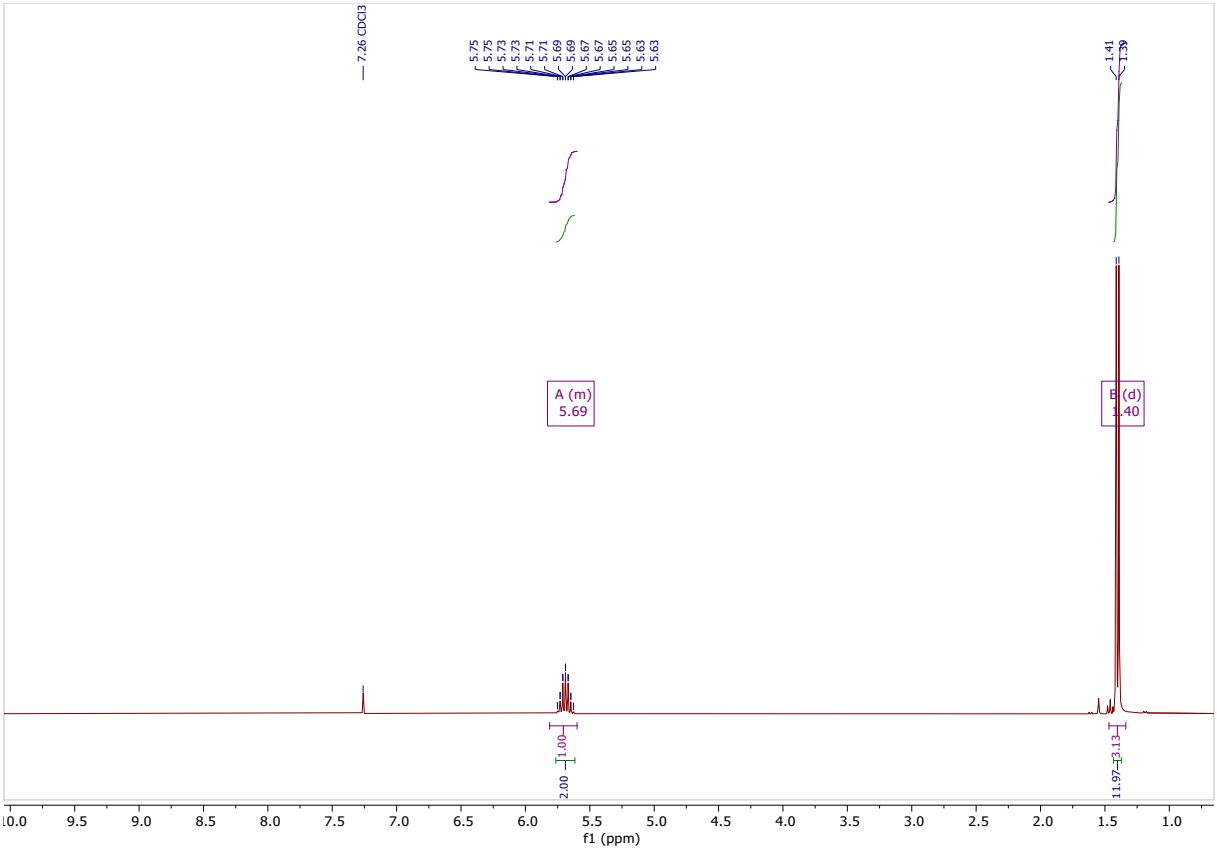

Figure S 7. ^{1}H NMR of diisopropylxanthogen disulfide in $CDCl_3$.

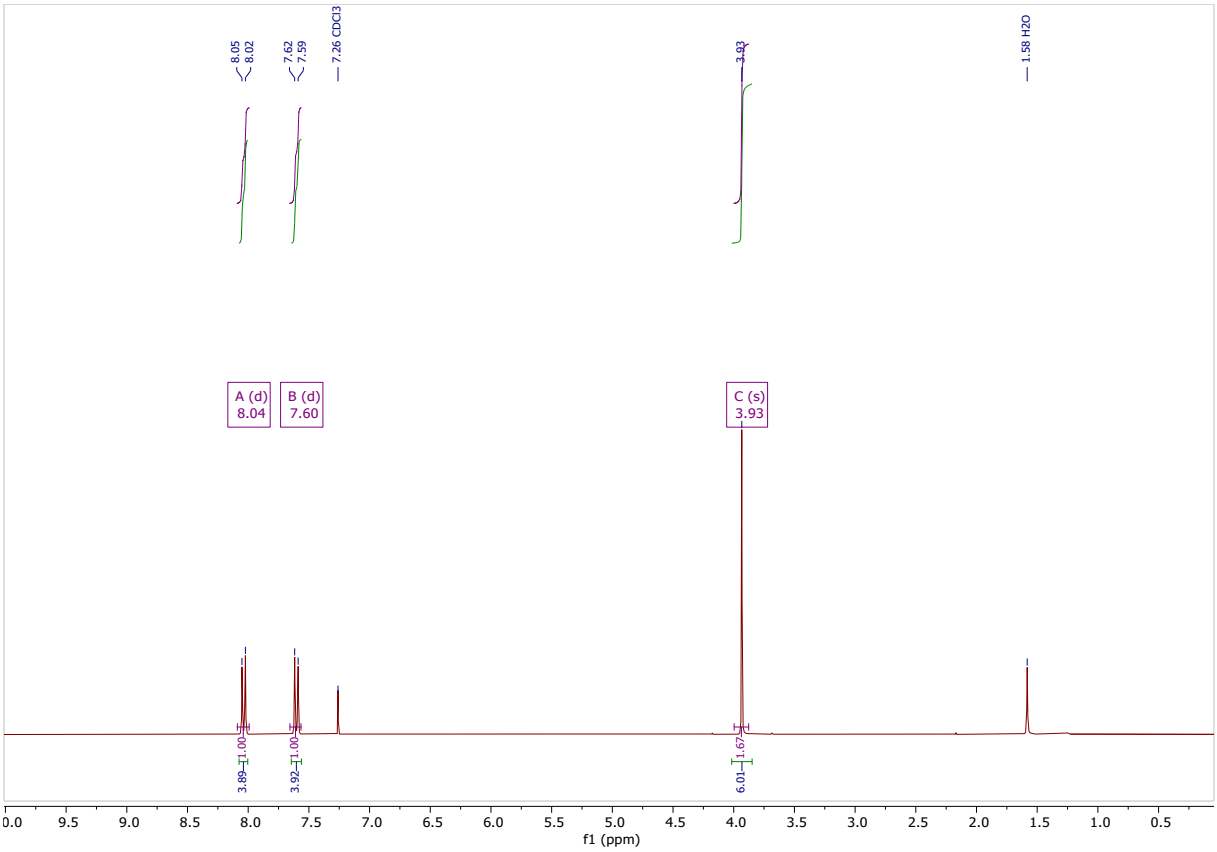

Figure S 8. ^{1}H NMR of dimethyl 4,4'-(ethyne-1,2-diyl)dibenzoate in $CDCl_3$.

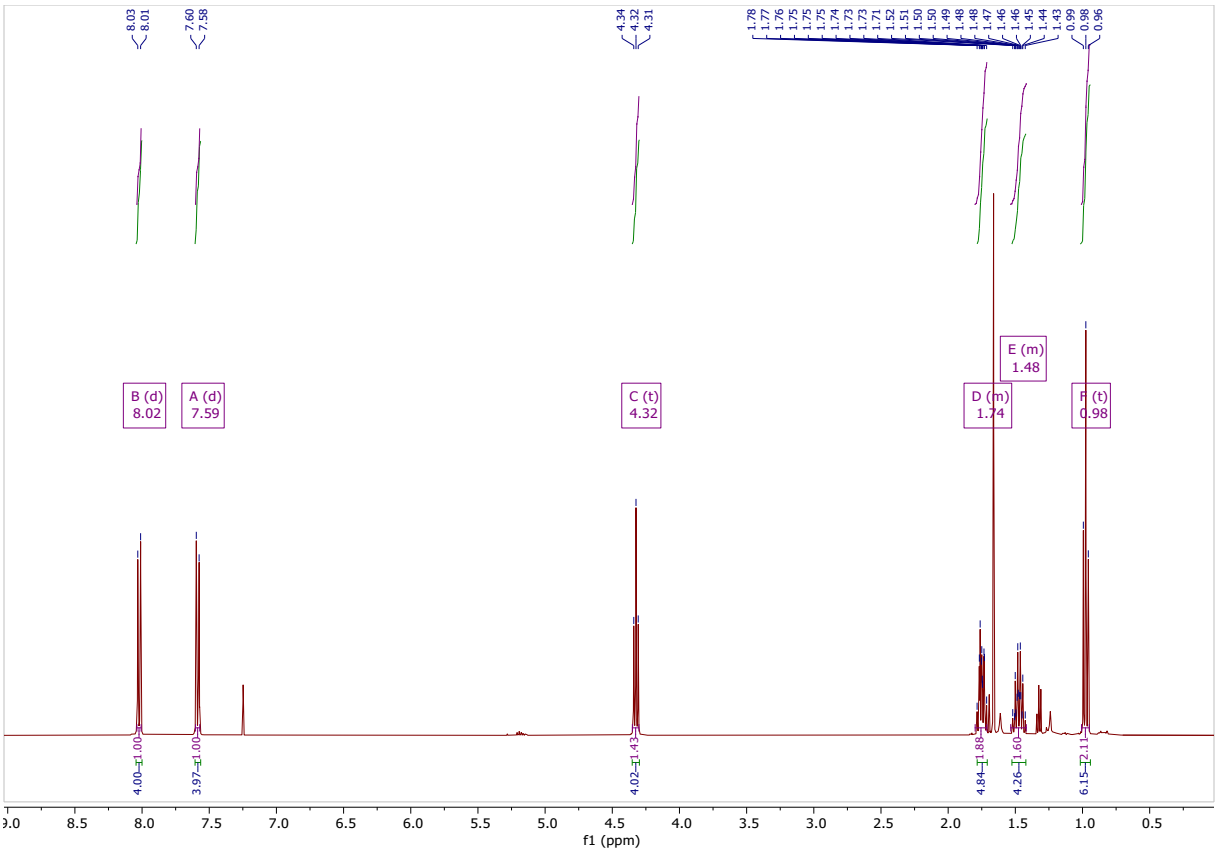

Figure S 9. ^{1}H NMR of **2** in $CDCl_3$.

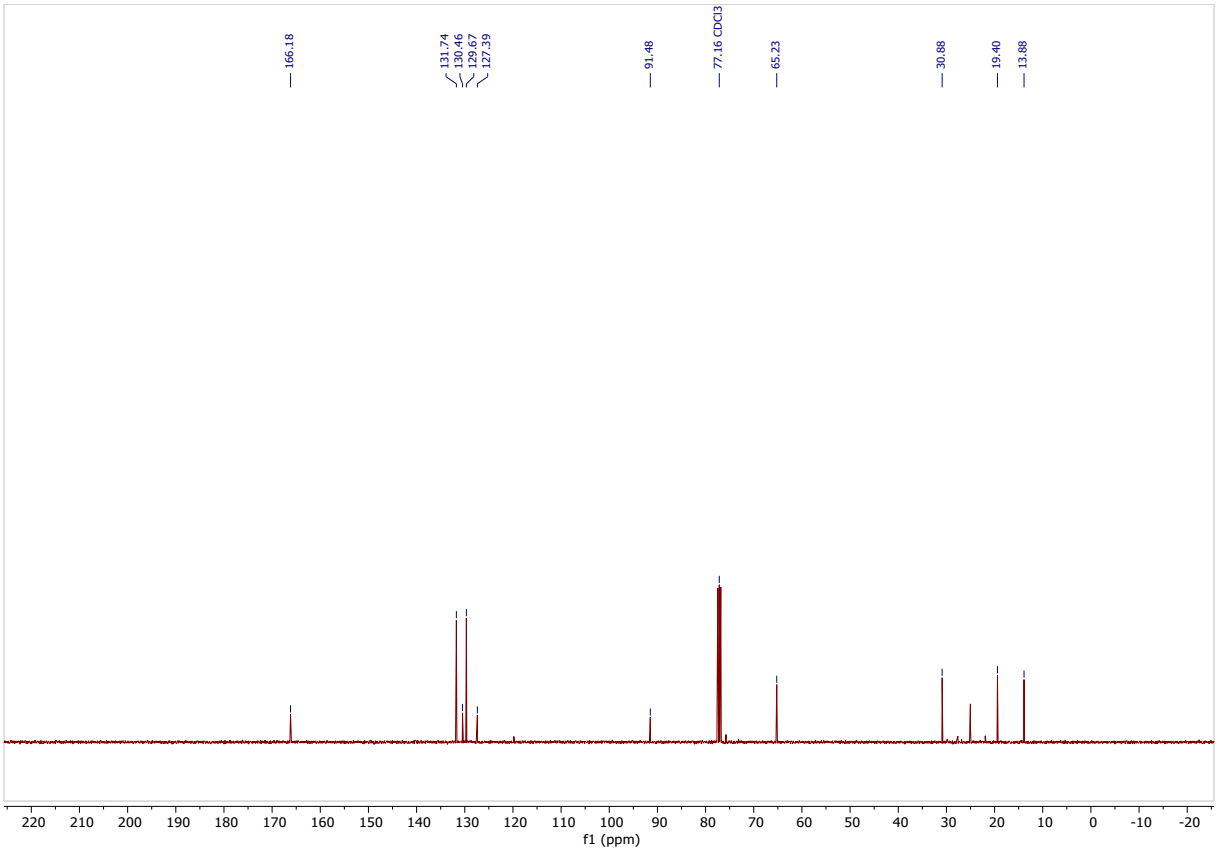

Figure S 10. ^{13}C NMR of **2** in $CDCl_3$.

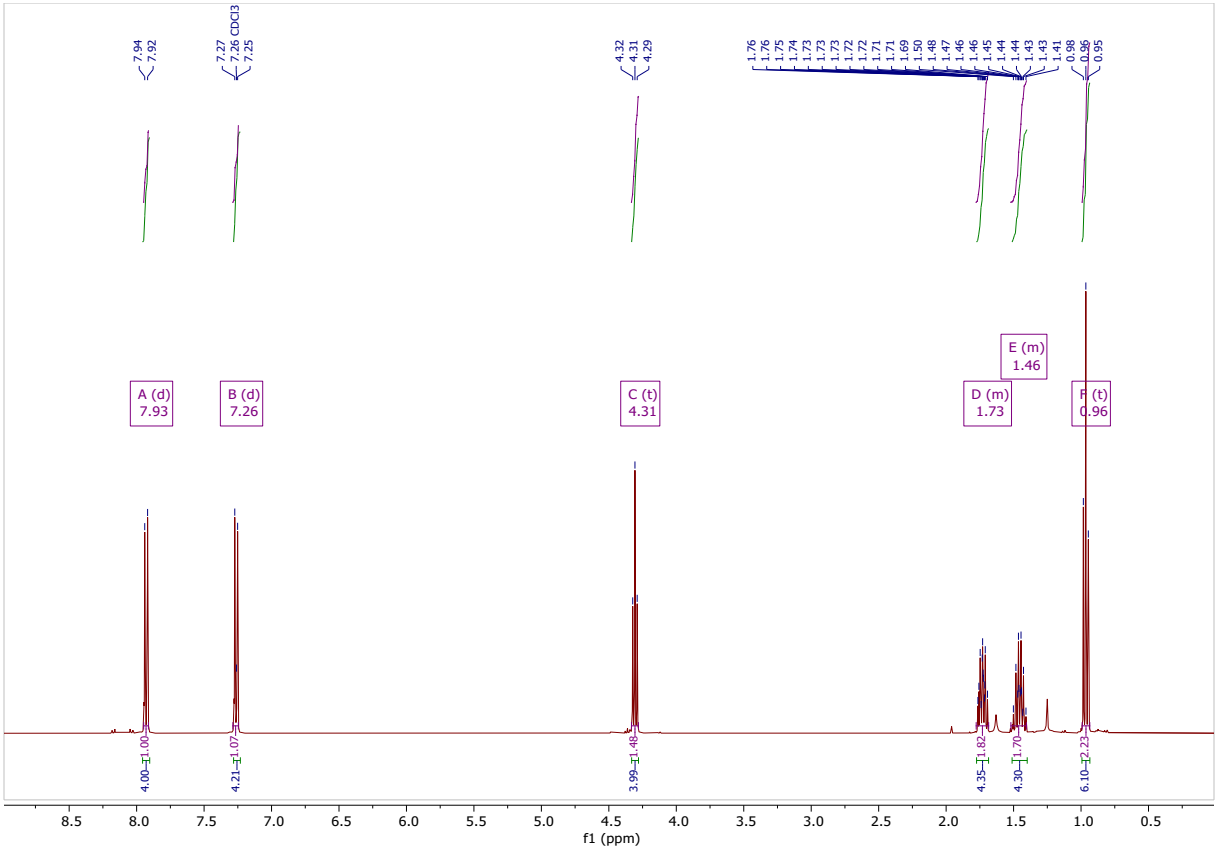

Figure S 11. ^{1}H NMR of **3** in $CDCl_3$.

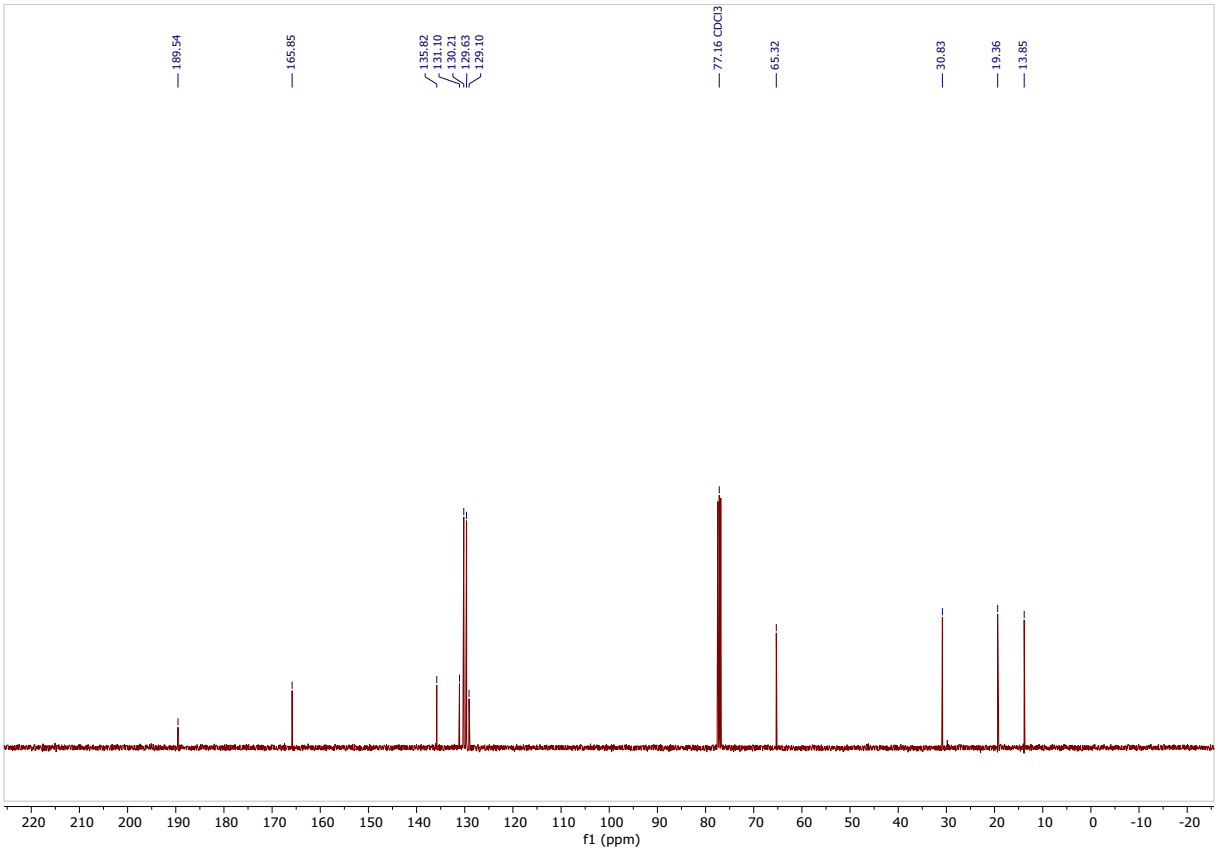

Figure S 12. ^{13}C NMR of **3** in $CDCl_3$.

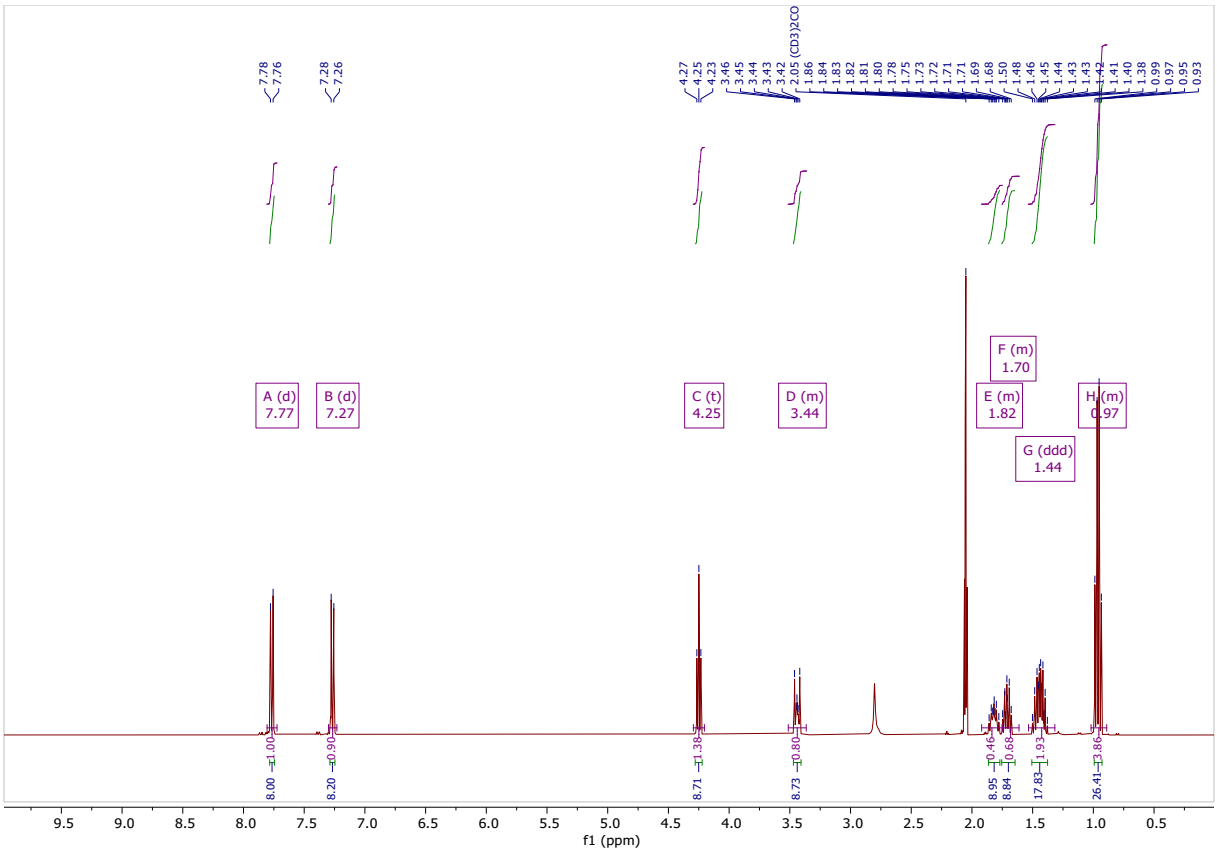

Figure S 13. ^{1}H NMR of **1-Bu$_4$(TBA)** in $(CD_3)_2CO$.

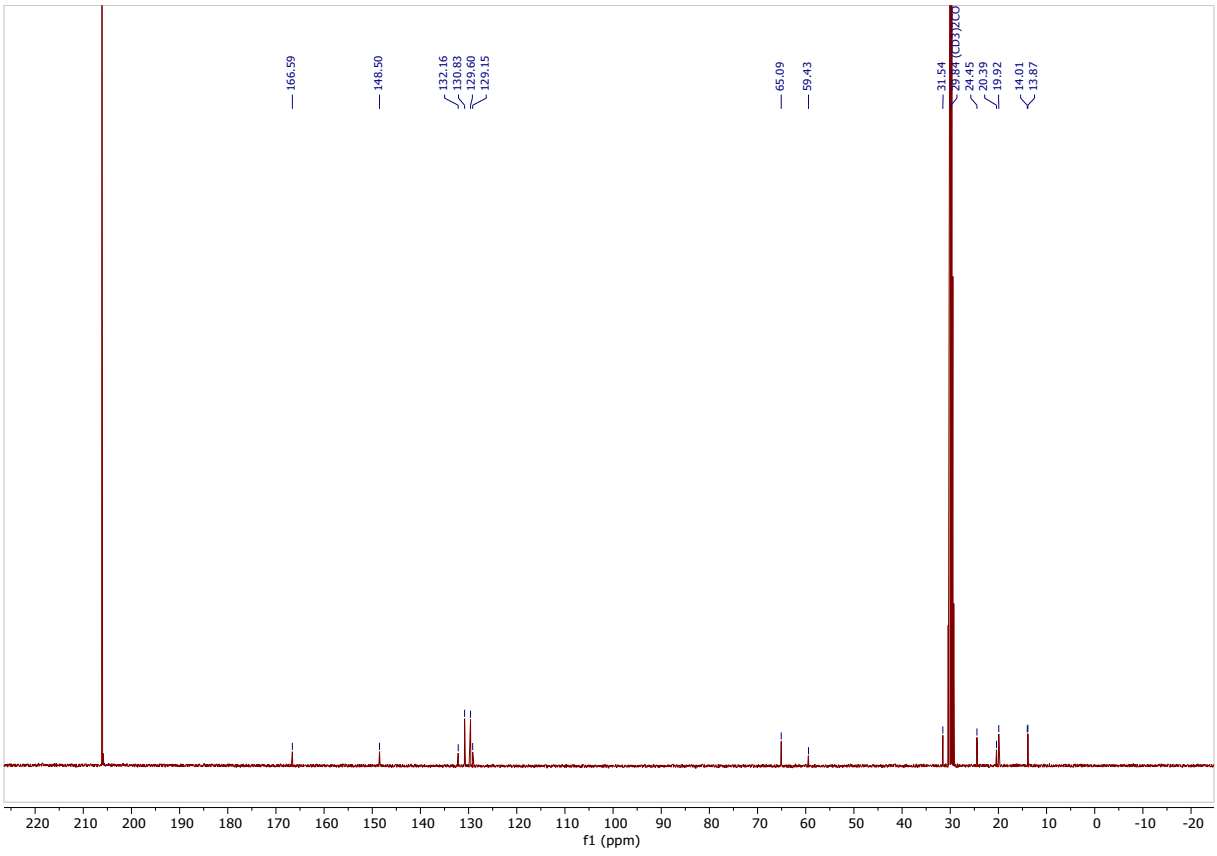

Figure S 14. ^{13}C NMR of **1-Bu$_4$(TBA)** in $(CD_3)_2CO$.

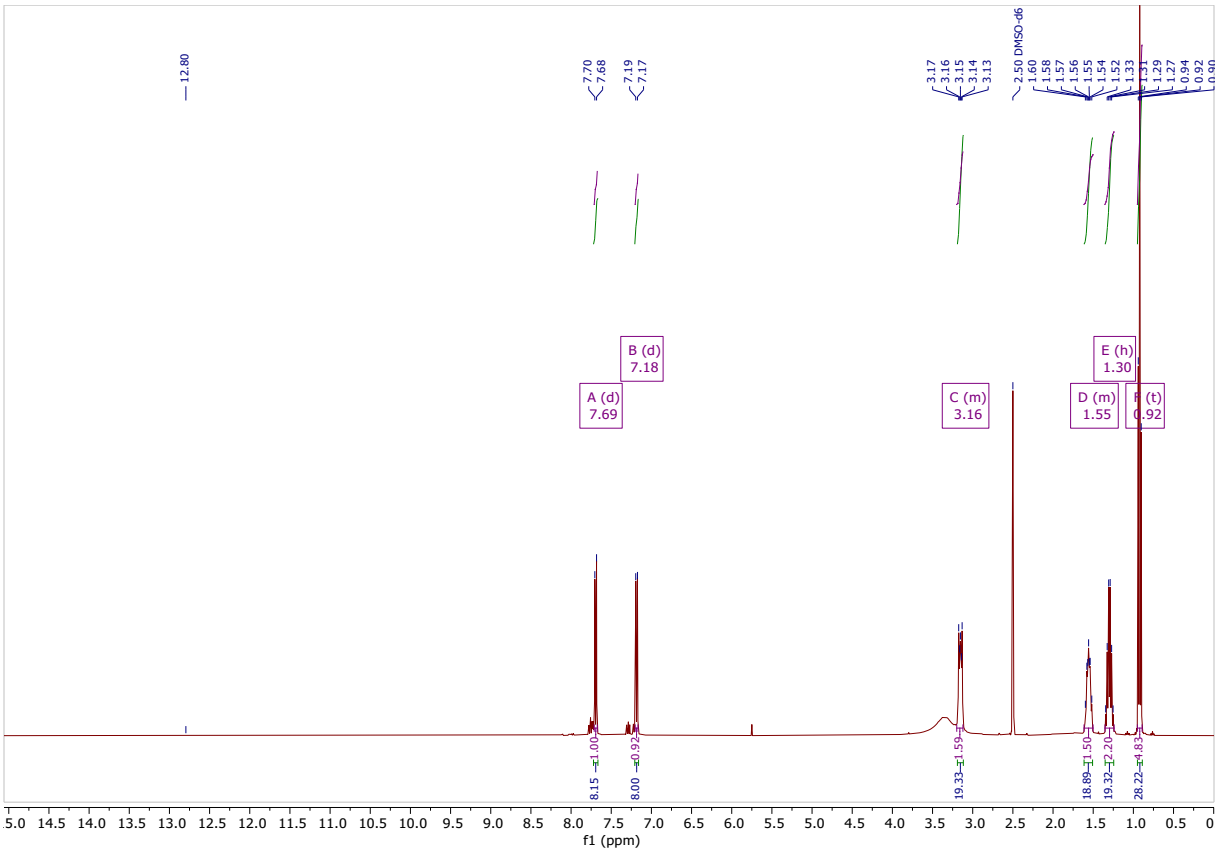

Figure S 15. ^{1}H NMR of **1-H$_3$(TBA)$_2$** in $(CD_3)_2SO$.

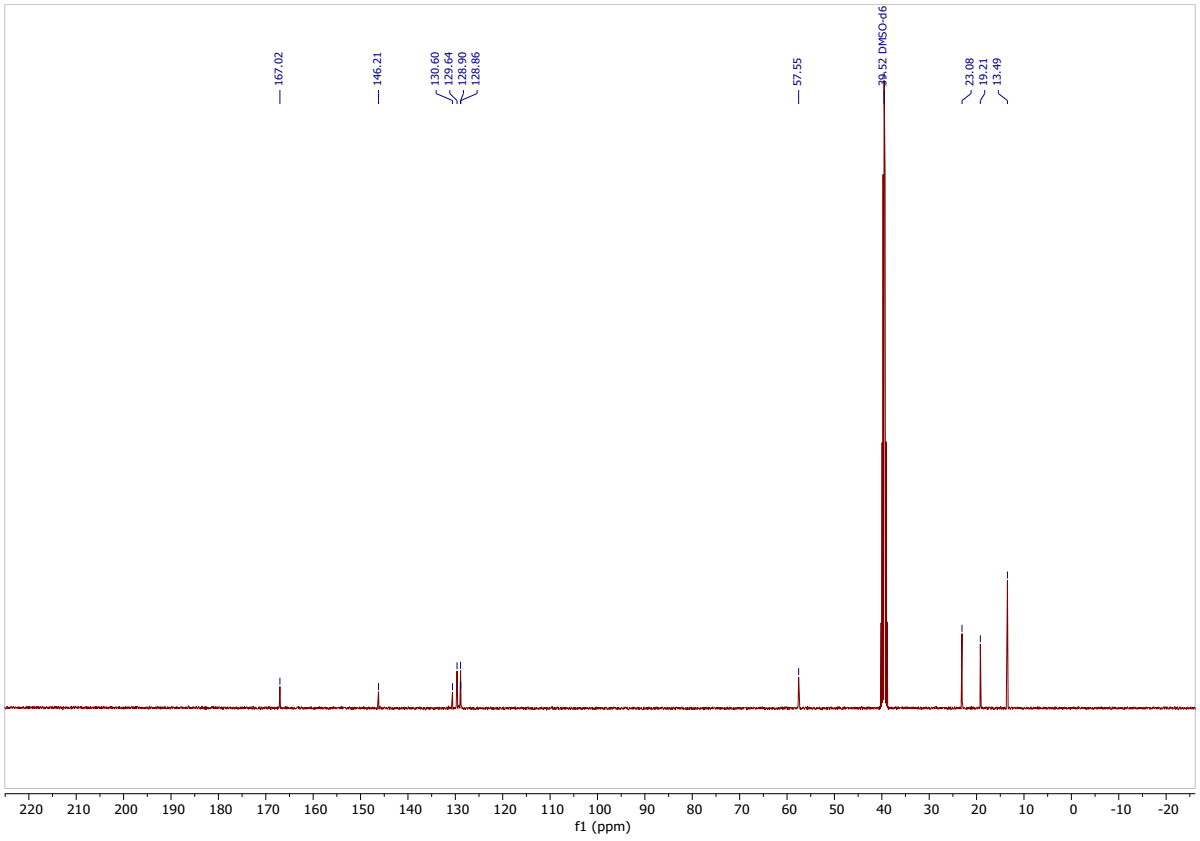

Figure S 16. ^{13}C NMR of **1-H$_3$(TBA)$_2$** in $(CD_3)_2SO$.

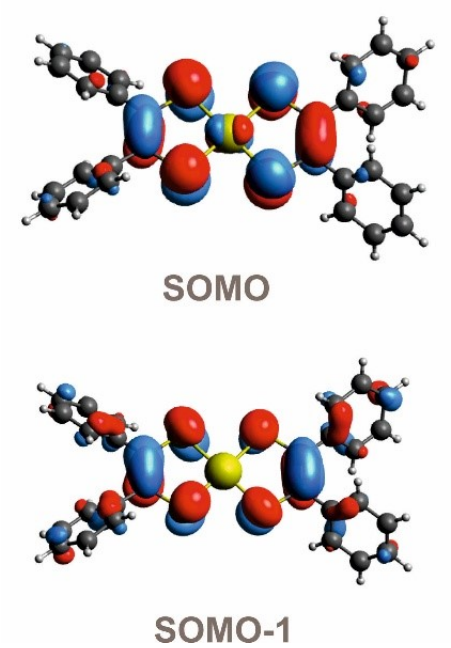

Figure S 17. SOMO and SOMO-1 for an Au bis(dithiolene) complex as in **1-H$_4$** where the carboxylic groups have been replaced by hydrogens. The yellow/black/grey spheres are the Au/C/H atoms (S atoms are not seen). The blue/red lobes are the positive/negative contributions to the molecular orbital.

Acknowledgements

This work was supported in France by the CNRS and the University of Angers. This work received financial support under the EUR LUMOMAT project and the Investments for the Future program ANR-18-EURE-0012 (support to Y.C. - MADCAP project). Work in Spain was supported by MCIN/AEI/10.13039/501100011033 and AEI through Grants PID2022-139776NB-C61 and PID2024-157317NB-I00 and by Generalitat de Catalunya (2021SGR01519 and 2021SGR00286). E.C. acknowledges MCIN/AEI/10.13039/501100011033 and AEI for support through the Severo Ochoa MATRANS42 (CEX2023-0001263-S) Excellence Centre distinction. P. A. acknowledges MCIN/AEI/10.13039/501100011033 and AEI for support through the Maria de Maeztu Units of Excellence Program (CEX-2021-001202-M).

References

1 G. M. Sheldrick, *Acta Crystallogr. A*, 2008, **64**, 112–122.
2 G. M. Sheldrick, *Acta Crystallogr. A*, 2015, **71**, 3–8.
3 C. B. Hübschle, G. M. Sheldrick and B. Dittrich, *J. Appl. Cryst.*, 2011, **44**, 1281–1284.
4 O. V. Dolomanov, L. J. Bourhis, R. J. Gildea, J. a. K. Howard and H. Puschmann, *J. Appl. Cryst.*, 2009, **42**, 339–341.